OncoTargets and Therapy

Dovepress
open access to scientific and medical research

Open Access Full Text Article

ORIGINAL RESEARCH

RETRACTED ARTICLE: Loss of miR-204-5p Promotes Tumor Proliferation, Migration, and Invasion Through Targeting YWHAZ/PI3K/AKT Pathway in Esophageal Squamous Cell Carcinoma

This article was published in the following Dove Press journal:
OncoTargets and Therapy

Zhimin Shen[1,*]
Tianci Chai[1,*]
Fei Luo[1]
Zhun Liu[1]
Hui Xu[1]
Peipei Zhang[1]
Mingqiang Kang[1–3]
Sui Chen[1]

[1]Department of Thoracic Surgery, Fujian Medical University Union Hospital, Fuzhou 350001, People's Republic of China; [2]Key Laboratory of Ministry of Education for Gastrointestinal Cancer, Fujian Medical University, Fuzhou 350001, People's Republic of China; [3]Fujian Key Laboratory of Tumor Microbiology, Fujian Medical University, Fuzhou 350122, People's Republic of China

*These authors contributed equally to this work

Purpose: MicroRNAs dysregulation has been confirmed in multiple malignancies. This paper reported the molecular mechanism of miR-204-5p in esophageal squamous cell carcinoma (ESCC).

Methods: miR-204-5p expression in 30 ESCC tumor tissues and 10 normal tissues was downloaded from RNA-seq data. ESCC tissues/normal tissues of 97 ESCC patients were collected. TE-1 and KYSE510 cells were transfected by miR-204-5p mimic, inhibitor, siYWHAZ or their corresponding controls. The phenotype of cells was detected by CCK-8 assay, transwell experiment, and flow cytometry. Luciferase reporter gene assay and RNA-binding protein immunoprecipitation (RIP) were performed to verify the targeting relationship between miR-204-5p and YWHAZ. miR-204-5p and YWHAZ expression in tissues/cells was detected by RT-PCR and Western blot. Xenograft tumor experiment was performed.

Results: miR-204-5p expression was declined in ESCC patients and cells, which was indicated to poor outcomes of patients. Compared with siNC group, TE-1 cells in miR-204-5p inhibitor group had higher OD450 value, less cell percentage in G1 phase, and more cell percentage in S phase, lower apoptosis percentage, and higher migration and invasion cell numbers. Moreover, KYSE510 cells of miR-204-5p mimic group showed lower OD450 value, more cell percentage in G1 phase and less cell percentage in S phase, higher apoptosis percentage, and lower migration and invasion cell numbers than control. YWHAZ was directly inhibited by miR-204-5p. Relative to siNC group, TE-1 cells of miR-inhibitor group exhibited higher YWHAZ protein expression, higher OD450 value, less cell percentage in G1 phase and more cell percentage in S phase, lower apoptosis percentage, higher migration and invasion cell numbers, and higher p-PI3K/PI3K and p-AKT/AKT protein expression, while siYWHAZ rescued the effects of miR-inhibitor. miR-204-5p up-regulation inhibited ESCC growth in vivo.

Conclusion: miR-204-5p inhibits ESCC progression by targeted inhibition of YWHAZ/PI3K/AKT.

Keywords: ESCC, progression, miR-204-5p, YWHAZ, PI3K/AKT

Introduction

Esophageal squamous cell carcinoma (ESCC) is a major common malignant tumor all over the world, which is identified as the sixth leading cause of cancer-related deaths.[1] As a distinct histological type of esophageal malignant tumor, the incidence of ESCC accounts for approximately 90% of the 456,000 esophageal cancer events per year,[2] and ESCC is usually diagnosed at advanced stage accompanied by regional or distant

Correspondence: Mingqiang Kang; Sui Chen
Department of Thoracic Surgery, Fujian Medical University Union Hospital, No. 29 Xinquan Road, Fuzhou 350001, People's Republic of China
Tel +86-18805910101; +86-13600867301
Email mingqiang_k068@163.com; chensui_567@163.com

metastases.[3] Complete surgical resection remains the main strategy for ESCC treatment, especially for advanced ESCC. However, despite advances have been made in recent years in the complete resections of ESCC, the prognosis of patients remains unsatisfactory due to the high incidence of local and distant failure.[4,5] Therefore, seeking a new direction for the treatment of ESCC is critical to improve patient prognosis.

In recent years, molecular-targeted therapy has made rapid progress and screening clinically applicable tumor-specific molecular biomarkers is crucial for the early detection and targeted therapy of this dreaded malignancy. MicroRNAs (miRNAs) are a family of small noncoding RNAs with 19–23 nucleotides in length.[6] MiRNAs have been shown to mediate post-transcriptional regulation of target genes through promoting RNA degradation or translational inhibition and participate in mediating various biological and pathological processes, including proliferation, apoptosis, differentiation, and carcinogenesis.[7] So far, many miRNAs have been confirmed to be involved in the development of ESCC. For instance, miR-141-3p and miR-25 were found to be up-regulated in ESCC, which acted as oncogenes in ESCC.[8,9] On the opposite, miR-214, miR-34a, and miR-138, which were down-regulated in ESC were considered as tumor suppressors in ESCC.[10–] MiRNAs are thus considered to be promising tumor markers and targets for the diagnosis and treatment of ESCC.

miR-204-5p has been confirmed to involve in the regulation of multiple human malignant tumor progression, which was also verified to be tumor suppressor in some human tumors such as malignant melanoma and hepatocellular cancer.[13,14] Unfortunately, the function of miR-204-5p in ESCC has not been confirmed currently. We hypothesized that miR-204-5p might participate in the regulation of ESCC progression. Thus, this paper has conducted sufficient studies to verify this hypothesis. Meanwhile, we also noticed that miR-204-5p directly targets YWHAZ. It is well known that YWHAZ is an important tumor regulator.[15] Therefore, this article further investigated whether miR-204-5p regulated the progression of ESCC via interfering with YWHAZ expression. This article might provide a potential target for the treatment of ESCC.

Methods

RNA-Seq Data

RNA-seq data of GSE114110 were downloaded from Gene Expression Omnibus (GEO, http://www.ncbi.nlm.nih.gov/geo/) database. In the GSE114110 database, 30 ESCC tumor tissues and 10 normal tissues were included.

Clinical Specimen

Tumor tissues and adjacent normal tissues of 97 ESCC patients stored in Fujian Medical University Union Hospital were obtained. All included patients were firstly diagnosed with ESCC in Fujian Medical University Union Hospital from May 2012 to Nov. 2018, which had no history of treatment for any other cancer-related diseases. The ESCC clinical pathology of all patients was recorded, including age, gender, tumor location, tumor size, TNM stage, and lymph node metastasis. The correlation between miR-204-5p expression and ESCC clinical pathology was analyzed.

This study has obtained written informed consent from all participants and has been approved by ethics committee of Fujian Medical University Union Hospital. Our study was conducted in accordance with the Declaration of Helsinki.

Cell Culture

Human esophageal epithelial cell line (Het-1A) and 5 ESCC cell lines (TE-1, ECA109, EC9706, KYSE410 and KYSE510) were obtained from Shanghai Institutes for Biological Sciences, Chinese Academy of Sciences (Shanghai, China). Each cell line was separately maintained in dulbecco's modified eagle medium (DMEM) containing 10% fetal bovine serum (FBS) in a constant temperature incubator at 37°C, 5% CO_2.

Cell Transfection

TE-1 and KYSE510 cells were harvested and seeded in 6-well plates with 1 mL of DMEM without FBS. Totally 1×10^5 cells were seeded in each well. miR-204-5p inhibitor and corresponding negative control were transfected into TE-1 cells (named miR-204-5p inhibitor group and siNC group, respectively), while miR-204-5p mimic and corresponding negative control were transfected into KYSE510 cells (set as miR-204-5p mimic group and NC group, respectively). In addition, co-transfection was also performed on TE-1 cells. Based on the transfection, the cells were grouped into siNC, miR-inhibitor, miR-inhibitor+siCtrl, and si-inhibitor +siYHAZ groups. All stably transfected cells were screened and re-cultured in DMEM containing 10% FBS at 37°C, 5% CO_2. Lipofectamine 2000 (Invitrogen, USA) was used for transfection and all transfectants used in this study were purchased from GenePharma (Shanghai, China).

CCK-8 Assay

The proliferation ability of cells was assessed by CCK-8 assay. After transfection, TE-1 and KYSE510 cells were inoculated in triplicate in 96-well plates with 1×10^5 cells per well. DMEM with 10% FBS (100 μL) was contained in each well. Cells were incubated at 37°C, 5% CO_2 for 24, 48, and 72 h. Totally 10 μL of CCK-8 reagent was added into each well at each time point. Cells were then incubated for 4 h at room temperature. The optical density value (OD) of each well was subsequently detected by a microplate reader at 450 nm wavelength.

Cell Cycle

Cell cycle analysis was performed by flow cytometry assay. Briefly, those successfully transfected TE-1 and KYSE510 cells were fixed with ice-cold ethanol (75%) for 12 h. Then, propidium iodide (PI) staining solution was used to re-suspend these cells in darkness for 30 min. In the PI staining solution, PI (50 μg/mL), ribonuclease A (50 μg/mL), and Triton X-100 (diluted in phosphate-buffered saline, 0.2%) were contained. The cell cycle distribution was detected by a FACSCalibur Flow Cytometer (BD, USA) and data were processed by the Modfit software.

Apoptosis

The apoptosis of transfected TE-1 and KYSE510 cells was evaluated by Flow cytometry. In short, cells were collected after 48 h transfection and washed twice with ice-cold PBS. A total of 5 μL Annexin V-fluorescein isothiocyanate (FITC) (Thermo Fisher Scientific, USA) and PI were then added into cells strictly according to the instructions. A flow cytometer (Beckman Coulter, USA) was used to assess the apoptotic rate of cells, and data were analyzed by FlowJo software (FlowJo LLC, Ashland, OR, USA).

Transwell Experiment

The transfected TE-1 and KYSE510 cells were subjected to migration and invasion assays by using 24-well transwell chambers (8-μm pore size). A total of 5×10^4 cells dispersed in 100 μL of serum-free DMEM were added into the upper chamber. For invasion assay, 100 μg of Matrigel (BD, USA) was pre-spread into the upper chamber, whereas Matrigel was not needed for migration assay. DMEM with 10% FBS (500 μL) was contained in the bottom wells. Cells were incubated at 37°C, 5% CO_2 for 24 h. After scraping cells on the upper surface, cells on the lower surface were subjected to fixation with methanol and staining with 0.1% crystal violet. The number of cells on the lower surface was observed and counted under an inverted microscope (Olympus, Japan).

Luciferase Reporter Gene Assay

KYSE510 cells of miR-204-5p mimic group and NC group were seeded in 96-well plates. The YWHAZ-wild type (WT) and -mutant type (Mut) of the 3′UTR region was designed by GenePharma (Shanghai, China) and then cloned into the psiCHECK-2 luciferase reporter vector (Promega, USA). KYSE510 cells of the two groups were co-transfected with psiCHECK-2 luciferase reporter vector containing the YWHAZ-WT and -Mut. The firefly and Renilla luciferase activities of each group were detected by the Dual-Luciferase Reporter Assay Kit (Promega, USA) after 48 of co-transfection.

RNA-Binding Protein Immunoprecipitation (RIP)

KYSE510 cells were collected after washing twice with PBS. Cells were mixed with 10 mL of PBS and 0.01% of formaldehyde for 15 min. Glycine (2 mol/L, 1.4 mL) was subsequently added to the cells and then these cells were subjected to centrifugation for 5 min at 1500 r/min. After the supernatant was discarded, cells were washed twice with PBS and lysed using RIPA. The cell lysate was obtained and evenly divided into two groups (YWHAZ group and Ctrl group). For YWHAZ group, 4 μg of YWHAZ antibody was added while an equal amount of normal rabbit IgG was added into the Ctrl group for 12 h incubation at 4°C. Protein A resin with a volume of 20 μL was added to each group for 1 h incubation at 4°C. Centrifugation was performed on each group, the supernatant was discarded, and the Protein A resin was washed 4 times with PBS. A total of 50 μL PBS was used to re-suspension the Protein A resin of each group. The RNA in each group was extracted with TRIzol reagent, and miR-204-5p expression level was detected by qRT-PCR after reverse transcription.

Immunohistochemistry Assay

Specimens of esophageal squamous cell carcinoma and adjacent tissues were all fixed with 10% neutral formalin. After routine dehydration, the samples were embedded in paraffin and sectioned. 3% H_2O_2 was used to block endogenous peroxidase for 10 min. After PBS rinsing, wavelet antigen repair was performed. Normal goat serum was used to block for 30 min at room temperature to eliminate

non-specific staining. After incubation of the primary antibody (YWHAZ, p-PI3K, pI3K, p-AKT, and AKT) and related secondary antibodies, streptomycin was used for the biotinylated HRP complex and placed at 37° C for 30 min. Samples were processed at room temperature with DAB color development solution, and color development was controlled under a microscope. The samples were then dehydrated with gradient ethanol, transparented with xylene, and dried.

Xenograft Tumor in vivo

Animal researches in this study have been approved by the Animal Ethics Committee of Fujian Medical University Union Hospital. Animal experiments were performed in accordance with relevant guidelines and regulations of the Animal Care and Use Committees at the Fujian Medical University Union Hospital, and a signed document issued by the Animal Care and Use Committees that granted approval was obtained.

Nude mice (n = 12, 4 weeks old) were provided by Shanghai Experimental Animal Center, Chinese Academy of Sciences (Shanghai, China), and they were randomly divided into miR-204-5p mimic group (n = 6) and NC group (n = 6). All mice were free to access to food and wat

KYSE510 cells transfected by miR-204-5p mimic o negative control were, respectively, subcut eously injected into the back of mice. A total of 6 × 10 cells were injected into each mouse. Every 3 ays, 30 g of Lipofectamine 2000-encapsulated mi -204- imic or negative control was, respectively jected into ouse of each group at the original injec on sit The tumor ength (L) and width (D) were easured eve 7 days using a digital caliper. The tu or volume was calculated with the following formula: V = (L × D^2)/2. On the 28th day after injection, all tumo issues ere obtained from mouse. The t mor w ight w eighted and expression of miR-20 5p and WHAZ in these xenograft tumor tissues was as ed by qRT-PCR and Western blot.

qRT-PCR

Total RNA in clinical specimen and cells were extracted by TRIzol reagent (Ambion, USA). According to the instructions, cDNA template was synthesized by the PrimeScriptTM RT reagent Kit (TaKaRa, Japan) with 1 μg of each RNA sample. Then, PCR amplification reaction was conducted by using the SYBR Green Real-time PCR Master Mix with the ABI PRISM 7500 Sequence Detection System (Applied Biosystems, USA). The PCR amplification reaction condition was set as follows: denaturation at 95°C for 5 min, followed by 40 cycles at 95°C for 15 s, 60°C for 15 s, and 72° C for 32 s. GAPDH and U6 was used as the internal control for YWHAZ and miR-204-5p. The primer sequences used in this research were listed as follows:

miR-204-5p-F, 5′-ACACTCCAGCTGGGTTCCCTTTG TCATCCTAT-3′, miR-204-5p-R, 5′-CTCAACTGGTGTCGT GGA-3′. YWHAZ-F, 5′-CCTCACTCCCGTTTCCG-3′, YW HAZ-R, 5′-CAGCACCTTCCGTCTTT-3′. GAPDH-F, 5′-AT GGGGAAGGTGAAGGTCG-3′, GAPDH-R, 5′-CTGGAAG ATGGTGATGGGA-3′. U6-F, 5′-CTCGCTTCGGCAGCAC A-3′, U6-R, 5′-AACGCTTCACGA TTGCC 3′.The rela-tive expression of miR-204-5p and WHAZ was e luated by the $2^{-\Delta\Delta CT}$ method.

Western Blot

Clinical specimen as grou into pow er in liquid nitrogen and then lysed sis buffer t b n total proteins of each sample. Total protei in cells were also harvested by using lysis b f The concen ation of each protein sample was mea ured using BCA Protein Assay kit (Beyotime, Jiangsu, Chi a). A total of 0 μg of each protein sample was separated using odium de ecyl sulfate-polyacrylamide gel electrophoresis PAGE). The separated proteins were transfe to a polyvinylidene fluoride (PVDF) membrane for h, and then the membrane was blocked with 5% skimmed milk at room temperature. Human monoclonal primary WHAZ antibody (1:1000, Santa Cruz, USA) was used to incubate the PVDF membrane overnight at 4°C. The PVDF membrane was further subjected to incubation with horseradish peroxidase (HRP)-conjugated secondary antibody (1:2000, Boster, Wuhan, China) for 2 h at room temperature. The blot of YWHAZ protein was detected by the Fluor ChemFC2 Imaging System (Alpha Innotech, SanLeandro, CA, USA). GAPDH was set as the internal control in this research.

Statistical Analysis

All experiments were performed in triplicate independently. All analyses were conducted using SPSS19.0 software and data were expressed in the form of mean ± standard deviation (M ± SD). Kaplan–Meier method was used for survival analysis. Correlation between two gene expression levels was analyzed using Pearson's Correlation Analysis. Comparison between two groups was assessed by Student's *t*-test, while that among more than two groups was estimated with ANOVA test. $P< 0.05$ was considered statistically significant.

Results

miR-204-5p Expression Was Declined in ESCC

One map of data from GEO database (GSE114110) was downloaded in order to explore the differential miRNA expression between ESCC tumor tissues and normal tissues (Figure 1A). In the database, 10 normal tissues and 30 ESCC tumor tissues were included. As shown in Figure 1B, miR-204-5p expression was significantly declined in ESCC tumor tissues when compared with normal tissues ($P< 0.001$). The expression of miR-204-5p in tumor and normal tissues of 97 ESCC patients was subsequently validated. It could be noted that relative to normal tissues, the expression of miR-204-5p was prominently reduced in ESCC tumor tissues ($P< 0.0001$) (Figure 1C). The correlation between miR-204-5p expression and ESCC clinical pathology was also analyzed. As recorded in Table 1, low miR-204-5p expression was obviously associated with large tumor size and advanced tumor stage ($P< 0.05$). Kaplan–Meier method was used for survival analysis. Interestingly, patients with lower expression of miR-204-5p were always with short overall survival time (Figure 1D).

Overexpression of miR-204-5p Suppressed ESCC Cells Proliferation, Migration, Invasion, and Enhanced Apoptosis

miR-204-5p expression in Het-1A cells and 5 ESCC cell lines (TE-1, ECA109, EC9706, KYSE410, and KYSE510) was investigated by qRT-PCR. The results are shown in Figure 2A. miR-204-5p expression was noticeably reduced in the 5 ESCC cell lines than that in Het-1A cell line ($P< 0.01$). In the next study, the biological functions of miR-204-5p in ESCC were analyzed. Briefly, TE-1 cells with relatively high miR-204-5p expression were tra[illegible]ected by miR-204-5p inhibitor, whereas KYSE510 cells [illegible]th relatively low miR-204-5p expression were transfected by mi[illegible]204-5p mimic. As shown in Figure 2B, TE-1 c[illegible]s in miR-20[illegible]5p inhibitor group had lower miR-204-5p expressi[illegible] than siNC group ($P< 0.01$), whereas KYSE510 ce[illegible]n miR-20[illegible]-5p mimic group were with higher miR-204-5p e[illegible]ression than NC group ($P< 0.01$). Thus, TE-1 and KYSE510 cells were both successfully transfected. CCK-8 assay showed markedly higher OD450 value of TE-1 cells in miR-204-5p inhibitor group when compared with siNC group ($P< 0.01$), but remarkably lower OD450 value of KYSE510 cells in miR-204-5p mimic group

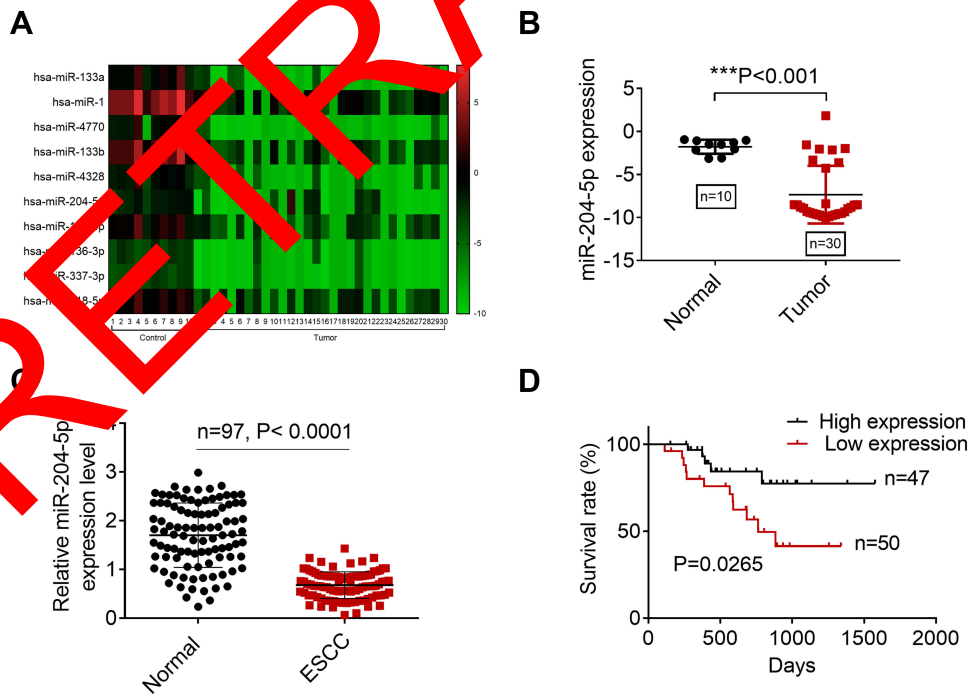

Figure 1 miR-204-5p expression was declined in ESCC. (**A**) Heat map of hierarchical clustering analysis. MiRNAs that were down-regulated were shown from red to green. (**B**) In the GEO database (GSE114110), 10 normal tissues and 30 ESCC tumor tissues were included. miR-204-5p expression was significantly declined in ESCC tumor tissues when compared with normal tissues. (**C**) Relative to normal tissues, the expression of miR-204-5p was prominently reduced in ESCC tumor tissues of 97 patients. (**D**) Kaplan–Meier method was used for survival analysis. ***$P< 0.001$.

Table 1 The Correlation Between miR-204-5p Expression and ESCC Clinical Pathology

Characteristics	Number of Patients	miR-204-5p Low Expression (≤Median)	miR-204-5p High Expression (>Median)	P value
Number	97	50	47	
Age				0.451
<60	45	24	21	
≥60	52	26	26	
Gender				0.096
Female	46	20	26	
Male	51	30	21	
Tumor location				0.336
Upper	31	16	15	
Middle	33	20	13	
Lower	33	14	19	
Tumor size				0.044
≤3 cm	44	18	26	
>3 cm	53	32	21	
TNM stage				0.025
I–II	52	22	30	
III–IV	45	28	17	
Lymph node metastasis				0.544
Yes	50	26	24	
No	47	24	23	

compared to NC group ($P< 0.01$) (Figure 2C). Moreover, TE-1 cells of miR-204-5p inhibitor group exhibited less cell percentage in G1 phase and more cell percentage in S phase than siNC group ($P< 0.05$ or $P< 0.01$). However, relative to NC group, KYSE510 cells of miR-204-5p mimic group showed more cell percentage in G1 phase and less cell percentage in S phase ($P< 0.01$) (Figure 2D).

In addition to proliferation and cycle, cell apoptosis, migration, and invasion were also detected. Compared with siNC group, much lower apoptosis percentage and higher migration and invasion cell numbers were observed in miR-204-5p inhibitor group ($P< 0.05$ or $P< 0.01$). On the opposite, relative to NC group, KYSE510 cells of miR-204-5p mimic group showed dramatically higher apoptosis percentage and lower migration and invasion cell numbers ($P< 0.01$) (Figure 2E and F).

YWHAZ Was Directly Inhibited by miR-204-5p and Was Highly Expressed in ESCC

The binding site of miR-204-5p and YWHAZ was predicted by TargetScan online software. The results indicated that miR-204-5p was with the binding site to YWHAZ in the 3′-UTR region. Then, YWHAZ-WT and YWHAZ-Mut containing the binding site were designed and synthesized (Figure 3A). Results of the luciferase reporter gene assay showed that miR-204-5p overexpression significantly decreased the relative luciferase activity of YWHAZ-WT ($P< 0.01$) whereas no obvious effect was found in YWHAZ-Mut group (Figure 3B). Thus, YWHAZ expression was proved to be directly inhibited by miR-204-5p. Meanwhile, much higher miR-204-5p enrichment was exhibited in YWHAZ group than that in Ctrl group ($P< 0.01$), which further confirmed that YWHAZ was directly bound to miR-204-5p (Figure 3C). Subsequently, YWHAZ expression in clinical tissues was detected. Compared with the relative YWHAZ expression in normal tissues, it was markedly increased in the ESCC tumor tissues ($P < 0.0001$) (Figure 3D). In ESCC tumor tissues, the YWHAZ expression level was prominently negatively correlated with the miR-204-5p expression ($P < 0.0001$) (Figure 3E). Based on the results of immunohistochemistry assay, YWHAZ expressed higher in tumor tissues than control (Figure 3F). Furthermore, the YWHAZ protein expression in the 5 ESCC cell lines was dramatically higher than that in Het-1A cell line ($P< 0.01$) (Figure 3G).

miR-204-5p Suppressed ESCC Development by Inhibiting YWHAZ/PI3K/AKT

Rescue assay included siNC, miR-inhibitor, miR-inhibitor +siCtrl, and si-inhibitor+siYHAZ groups. After transfection, the relative YWHAZ protein expression of TE-1 cells in miR-inhibitor group and that in si-inhibitor+siYHAZ groups were higher compared with that in siNC group ($P< 0.01$). However, siYWHAZ rescued the effects of miR-inhibitor, which significantly decreased YWHAZ expression ($P< 0.01$) (Figure 4A). The TE-1 cells phenotype was analyzed after co-transfection. As shown in Figure 4B–E, miR-inhibitor could improve proliferation, cell cycle, migration and invasion, and inhibit cell apoptosis of TE-1 cells. However, when siYWHAZ was co-transfected, these progresses were rescued (Figure 4B–E). Western blot analysis was processed to detect the relative protein expression of p-PI3K/PI3K and p-AKT/AKT. As the results shown in Figure 4F, relative protein expression of p-PI3K/PI3K and p-AKT/AKT was significantly higher in miR-inhibitor and miR-inhibitor+siCtrl than control, while siYWHAZ rescued the effect of miR-inhibitor. Thereby, down-regulated miR-204-5p improved the progress

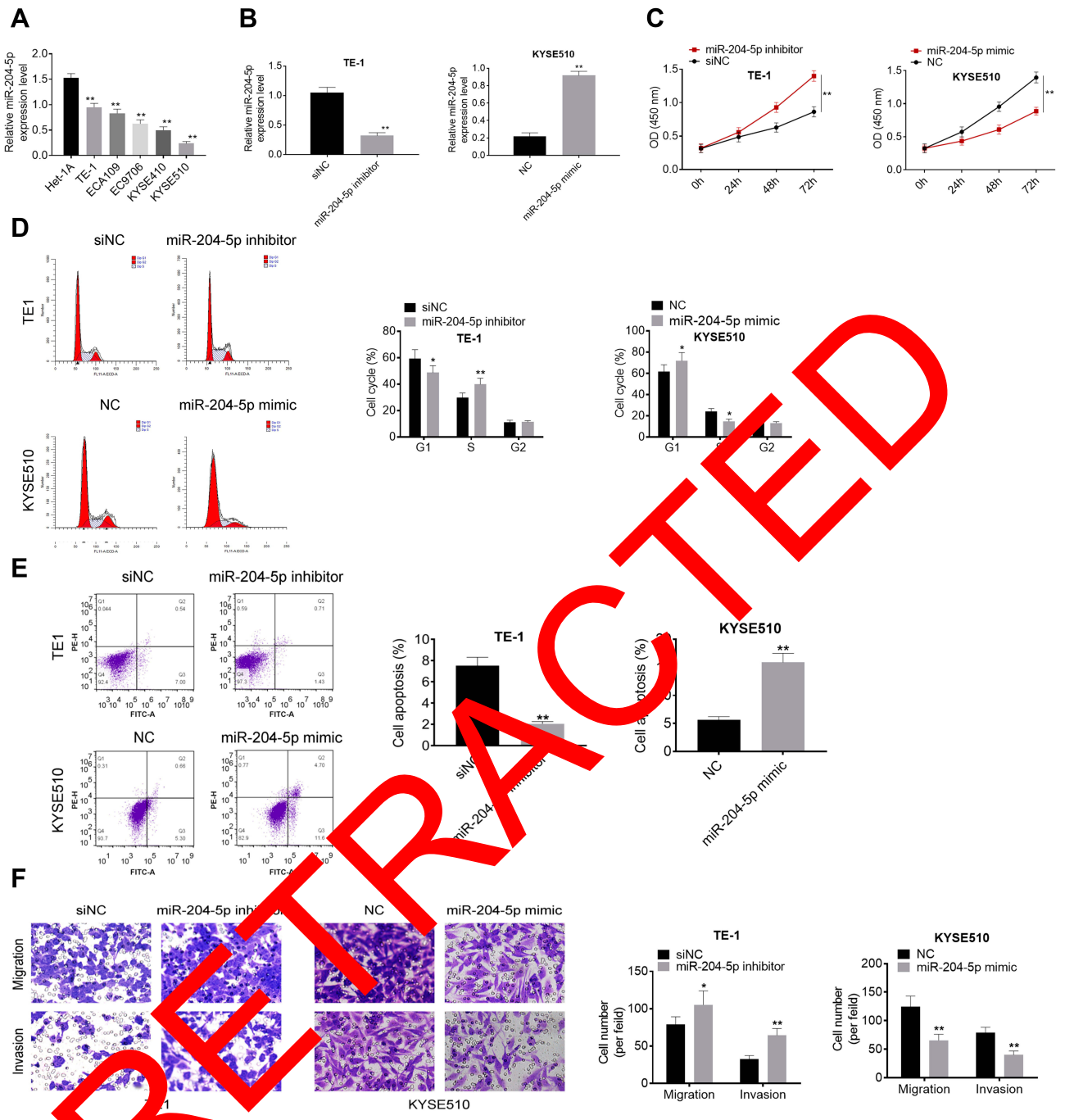

Figure 2 Overexpression of miR-204-5p suppressed ESCC cells proliferation, migration, invasion, and enhanced apoptosis. (**A**) miR-204-5p expression was noticeably reduced in 5 ESCC cell lines than that in Het-1A cell line. (**B**) TE-1 and KYSE510 cells were both successfully transfected. (**C**) Overexpression of miR-204-5p inhibited ESCC cell proliferation. (**D**) Overexpression of miR-204-5p arrested cell cycle in G1 phase. (**E**) Overexpression of miR-204-5p promoted ESCC cell apoptosis. (**F**) Overexpression of miR-204-5p suppressed ESCC cells migration and invasion. *P< 0.05. **P< 0.01.

of ESCC, while siYWHAZ could rescue the function of miR-inhibitor.

miR-204-5p Inhibited ESCC Growth in vivo by Suppressing YWHAZ Expression

The growth of xenograft tumors of ESCC in nude mice was measured. As shown in Figure 5A and B, both the tumor volume and weight of miR-204-5p mimic group were prominently lower than that of NC group on the 28th day after subcutaneous injection ($P < 0.01$). miR-204-5p and YWHAZ expression in tumor tissues of the two groups was then detected. As a result, tumor tissues of miR-204-5p mimic group exhibited much higher miR-204-5p expression and markedly lower YWHAZ expression than that of NC group

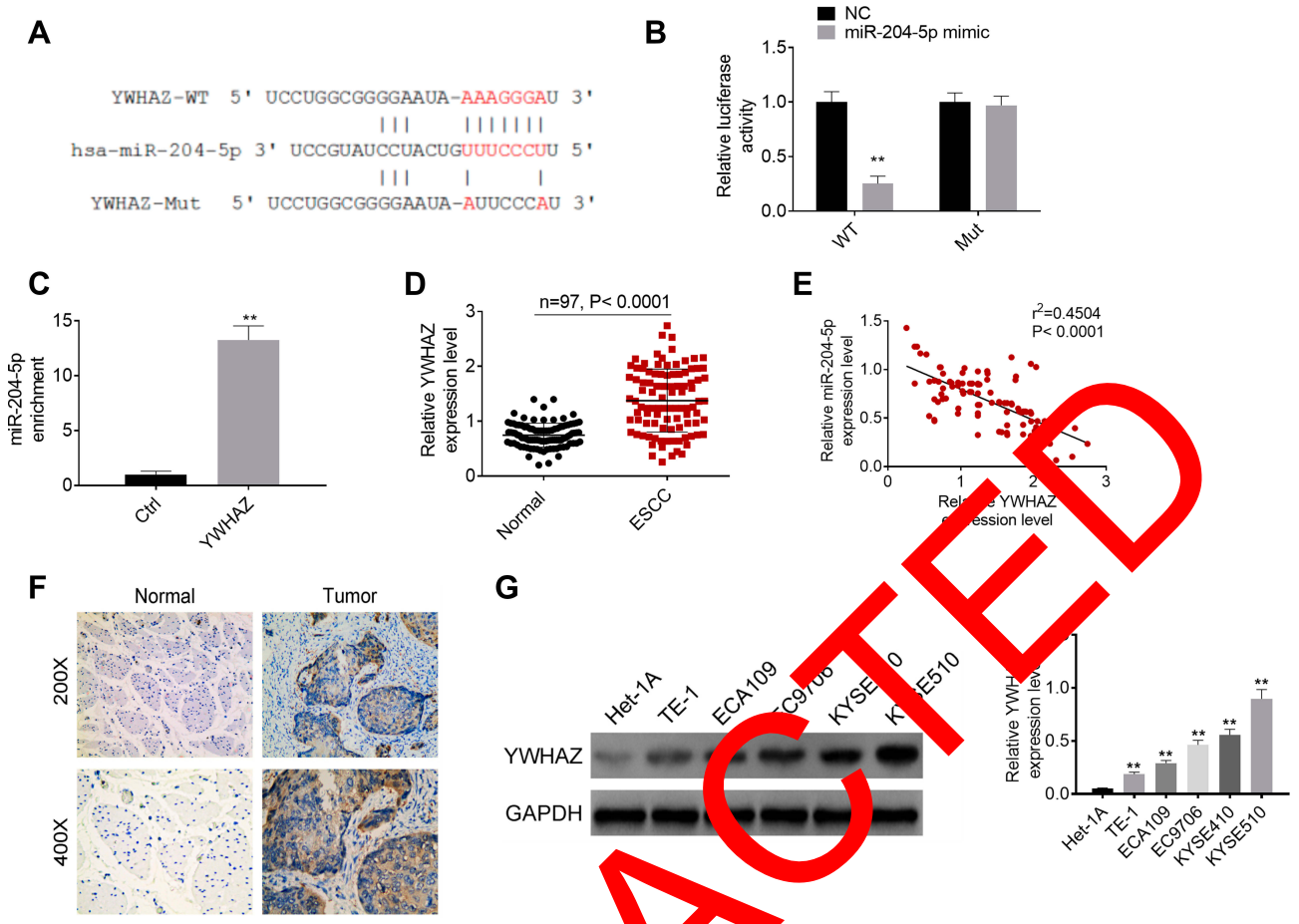

Figure 3 YWHAZ was directly inhibited by miR-204-5p and was highly expressed in ESCC. (**A**) YWHAZ-WT and YWHAZ-Mut containing the binding site were designed and synthesized. (**B**) Luciferase reporter gene assay showed that YWHAZ was directly inhibited by miR-204-5p. (**C**) Results from RIP exhibited much higher miR-204-5p enrichment in YWHAZ group than that in Ctrl group. (**D**) Compared with the relative YWHAZ expression in normal tissues, it was markedly increased in the ESCC tumor tissues. (**E**) In ESCC tumor tissues, the YWHAZ expression level was negatively correlated with the miR-204-5p expression level. (**F**) The expressions of YWHAZ were examined by IHC analysis. (**G**) YWHAZ protein expression in the 5 ESCC cell lines was dramatically higher than that in Het-1A cell line. ***P*< 0.01.

(*P*< 0.01) (Figure 5C and D). Immunohistochemistry assay also carried out for YWHAZ and the signaling markers. As shown in Figure 5E, the relative expression of YWHAZ, p-PI3K/PI3K, and p-AKT/AKT was significantly decreased after miR-204-5p mimic transfection.

Discussion

The tumorigenesis and development of ESCC are triggered by multiple factors. The abnormal expression of cancer-related genes will ultimately affect the development of tumors by inducing tumor growth, metastasis as well as a series of complex processes.[11] This research revealed that the down-regulated miR-204-5p expression in ESC indicated poor outcome of patients such as advanced stage and large tumor size. Regarding the mechanism, miR-204-5p inhibited ESCC progression in vitro and in vivo by targeting YWHAZ/PI3K/AKT.

The function of miR-204-5p in human malignancies has been reported in recent years. Previous research has reported that miR-204-5p expression was reduced in colorectal cancer. After restoring the expression of miR-204-5p, migration and invasion abilities of the colorectal cancer cells were weakened and the sensitivity of tumor cells to chemotherapy was also enhanced. The mechanism involved in this process was that miR-204-5p could directly inhibit RAB22A expression to exert its anti-tumor effect in colorectal cancer.[16] In papillary thyroid carcinoma, miR-204-5p possessed antitumor effect, which suppressed proliferation and induced apoptosis of papillary thyroid carcinoma cells by inhibiting the expression of IGFBP5.[17] miR-204-5p expression was also found to be markedly declined in hepatocellular cancer tissues and cells, and low miR-204-5p expression was associated with poor outcomes of hepatocellular cancer patients. miR-204-5p could inhibit hepatocellular cancer cells proliferation in vitro

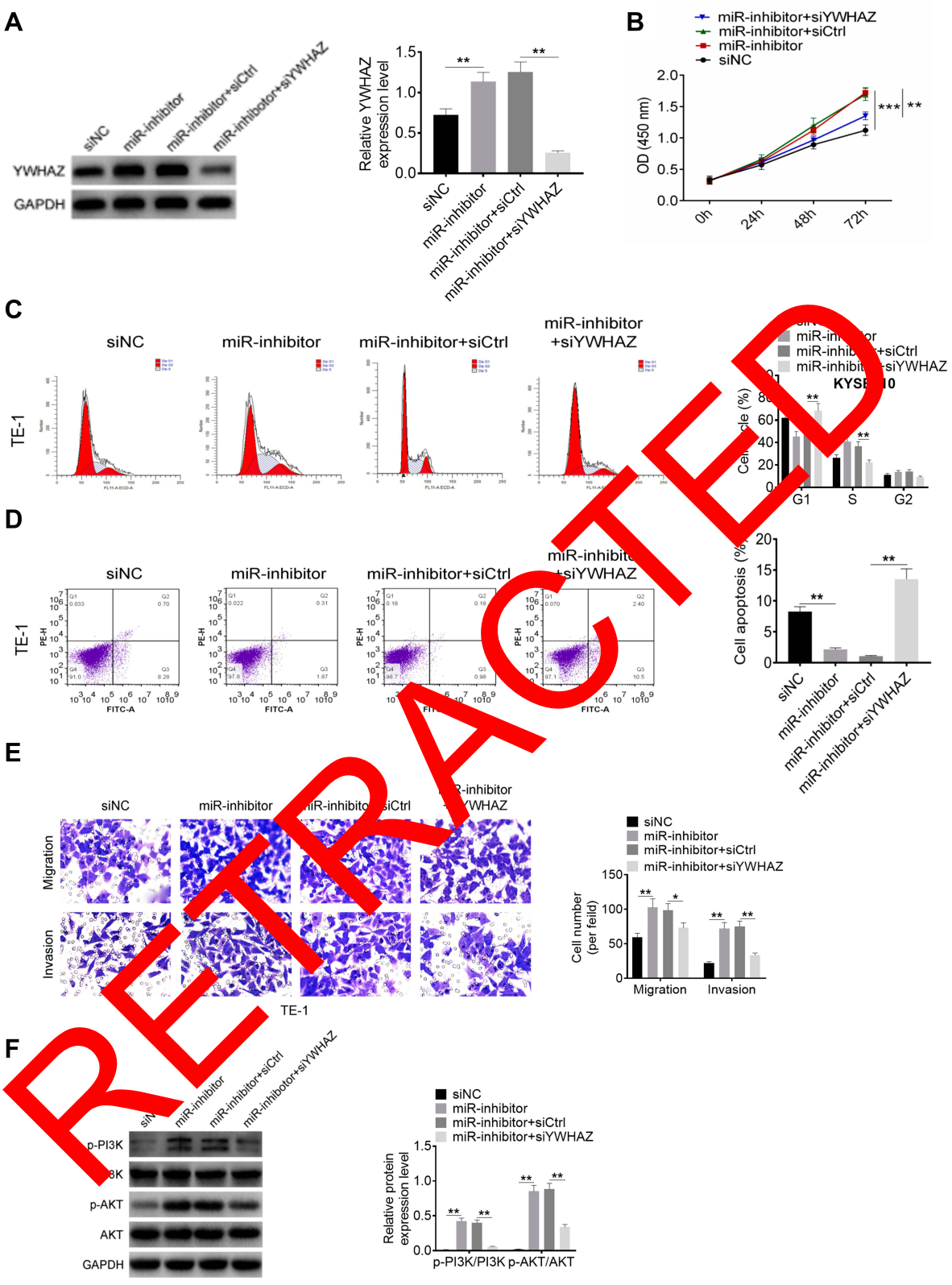

Figure 4 miR-204-5p suppressed ESCC development by inhibiting YWHAZ/PI3K/AKT. (**A**) Compared to siNC group, YWHAZ was expressed higher in miR-inhibitor and miR-inhibitor+siCtrl group, while it was lower expressed in miR-inhibitor+siYWHAZ. (**B**) The proliferation of TE-1 cells after siNC, miR-inhibitor, miR-inhibitor+siCtrl and si-inhibitor +siYHAZ transfection. (**C**) Remarkably less cell percentage in G1 phase and more cell percentage in S phase was observed in miR-inhibitor and miR-inhibitor+siCtrl group relative to siNC and miR-inhibitor + siYWHAZ group. (**D**) Lower apoptosis percentage was found in TE-1 cells of miR-inhibitor and miR-inhibitor+siCtrl compared with siNC and miR-inhibitor + siYWHAZ group. (**E**) Higher migration and invasion cell numbers were found in TE-1 cells of miR-inhibitor and miR-inhibitor+siCtrl group compared with that in siNC and miR-inhibitor + siYWHAZ group. (**F**) Relative to siNC and miR-inhibitor + siYWHAZ group, TE-1 cells of miR-inhibitor and miR-inhibitor+siCtrl had significantly higher p-PI3K/PI3K and p-AKT/AKT protein expression. *P< 0.05. **P< 0.01. ***P<0.001.

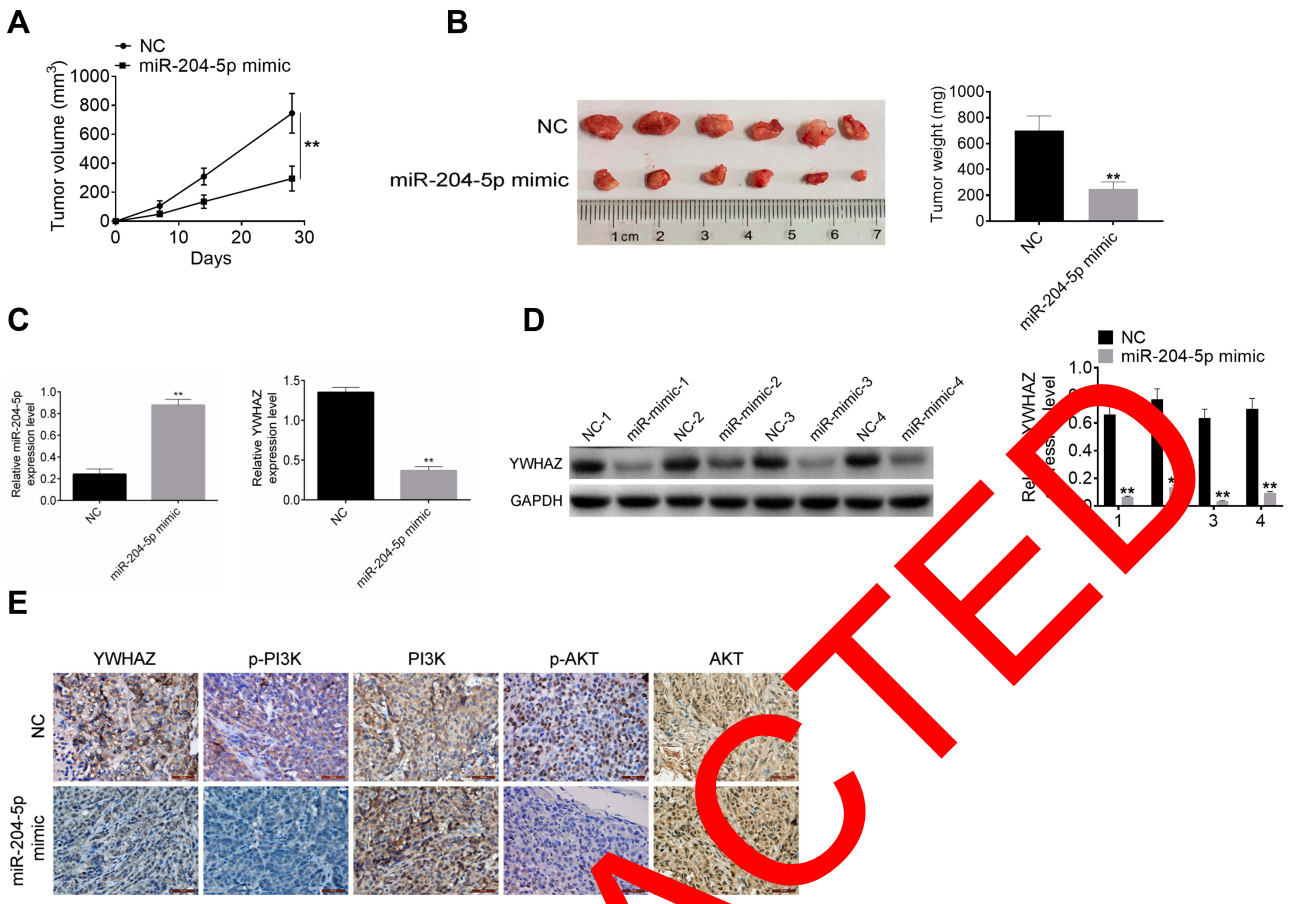

Figure 5 miR-204-5p inhibited ESCC growth in vivo by suppressing YWHAZ expr[illegible]. (**A**) The tumor volume of miR-204-5p mimic group was prominently lower than that of NC group on the 28th day after subcutaneous injection. [illegible]he 28th [illegible] after subcutaneous injection, the tumor weight of miR-204-5p mimic group was markedly lower than that of NC group. (**C**) Subcutaneous tum[illegible] tissues [illegible]miR-204[illegible] mimic group exhibited much higher miR-204-5p expression and markedly lower YWHAZ mRNA expression than that of NC group. (**D**) Sub[illegible]aneous tum[illegible] tissues of [illegible]R-204-5p mimic group showed markedly lower YWHAZ protein expression than that of NC group. (**E**) The results of immunohistochemistry [illegible]ved tha[illegible]pression of YWHAZ, p-PI3K/PI3K, and p-AKT/AKT was significantly decreased after miR-204-5p mimic transfection. **$P< 0.01$.

by regulating SIX1 and its down[illegible]ream g[illegible]es.[14] Meanwhile, Wang et al[18] reported that mi[illegible]204-5p was lo[illegible]r expressed in oral squamous cell carc[illegible]oma, a[illegible] miR-204-5p acted as a tumor suppressor in ora[illegible]uam[illegible]us cell carcinoma via targeting CXCR4. The[illegible] most [illegible]udies h[illegible]e suggested that miR-204-5p play[illegible] as a [illegible]mor su[illegible]ssor in multiple human malignant t[illegible]ors, S[illegible]these studies, this research also illustrated that [illegible]R-204-5p acted as a tumor suppressor in ESCC. More impor[illegible]tly, this study demonstrated for the first time that miR-204-5p inhibited ESCC progression via regulating YWHAZ/PI3K/AKT. These findings laid reliable theoretical basis for the application of miR-204-5p in the clinical target treatment of ESCC.

YWHAZ gene is located on chromosome 8q22.3, which encodes tyrosine 3-monooxygenase/tryptophan 5-monooxygenase activation protein, zeta (14-3-3 ζ).[19,20] YWHAZ has been shown to be overexpressed in a variety of cancer tissues and cell lines, which could be identifiedas a cancer-related prognostic marker.[15] YWHAZ also predicts poor prognosis of patients, such as pancreatic cancer, breast cancer, colon cancer, lung cancer, oral cancer, and esophagus cancer.[15] Watanabe et al[21] also demonstrated that YWHAZ was abnormally up-regulated in adenocarcinoma of the esophago-gastric junction and closely associated with lower overall survival, thereby it was considered as an independent prognostic factor for patients. Results from this data also indicated that YWHAZ expression was aberrantly up-regulated in ESCC and negatively correlated with the miR-204-5p expression. YWHAZ has been found to be directly regulated by miR-613, miR-22, miR-451, miR-30c in human hepatocellular carcinoma, colorectal cancer, and breast cancer.[22–25] This article proved for the first time that YWHAZ was directly inhibited by miR-204-5p in ESCC.

PI3K/AKT is an important cancer-related signaling pathway, which is participated in the regulation of several human tumor progression, including lung cancer, hepatocellular carcinoma, gastric cancer, bladder cancer, etc.[26–29] PI3K/AKT signaling pathway was also reported to be involved in the regulation of ESCC and the activation of PI3K/AKT signaling pathway was conducive to the growth and metastasis of ESCC.[30] PI3K/AKT signaling pathway can involve in regulating the cell cycle process. The activated AKT promotes the binding of cyclin D1 and cyclin-dependent protein kinase, thereby promoting the transition of the cell cycle from G1 phase to S phase and accelerating tumor development via shorting the cell cycle.[31,32] At the same time, the activated PI3K/AKT signaling pathway can inhibit apoptosis and promote cell survival via regulating the expression of apoptosis-related proteins, such as Bcl-2 and Bad.[33] In addition, angiogenesis is one of the important reasons for tumor growth and metastasis, and the activation of PI3K/AKT signaling pathway can inhibit normal blood vessel development and promote tumor angiogenesis.[34] In this research, miR-204-5p inhibited the development of ESCC partially through suppressing the activation of YWHAZ/PI3K/AKT.

Collectively, this article discovered that miR-204-5p expression was reduced in ESCC and overexpression of miR-204-5p could inhibit the progression of ESCC by targeting YWHAZ/PI3K/AKT signaling. Thus, miR-204-5p might be a novel potential target for the treatment of ESCC.

Highlights

(1) miR-204-5p expression was declined in ESCC.
(2) miR-204-5p overexpression suppressed ESCC development in vitro.
(3) YWHAZ was directly inhibited by miR-204-5p and was highly expressed in ESCC.
(4) miR-204-5p suppressed ESCC development by inhibiting YWHAZ/PI3K/AKT.
(5) miR-204-5p inhibited ESCC growth in vivo by suppressing YWHAZ expression.

Acknowledgments

This study was supported by National Natural Science Foundation of China (Grant number: 81773129) Joint Funds for The Innovation of Science and Technology, Fujian province (Grant numbers:2017Y9039 and 2018Y9034), Program for Innovative Research Team in Science and Technology in Fujian Province University and Startup Fund for scientific research, Fujian Medical University (Grant number: 2017XQ2027). Dr. Zhimin Shen and Dr. Tianci Chai are co-first authors for this study.

Disclosure

The authors report no conflicts of interest in this work.

References

1. Okuda M, Inoue J, Fujiwara N, et al. Subcloning and characterization of highly metastatic cells derived from human esophageal squamous cell carcinoma KYSE150 cells by in vivo selection. *Oncotarget*. 2017;8(21):34670–34677.
2. Abnet CC, Arnold M, Wei WQ. Epidemiology of esophageal squamous cell carcinoma. *Gastroenterology*. 2017;154(2):360–373.
3. Celik S, Mergan D, Dülger AC, et al. Are serum Mac 2-binding protein levels elevated in esophageal cancer? A control study of esophageal squamous cell carcinoma patients. *Dis Markers*. 2018;156(12):408–[illegible].
4. Wang L, Zhang H, [illegible] A, et al. Partitioning-defective 3 (PARD3) regulates proliferation, apoptosis, migration, and invasion in esophageal squamous cell carcinoma cells. *Med Sci Monit*. 2017;23:2382–2390.
5. Jiang Y, Lo CY, Wong A, et al. Prognostic significance of tumor-infiltrating immune cells and PD-L1 expression in esophageal squamous cell carcinoma. *Oncotarget*. 2017;8(18):30175–30189.
6. Fan X, Chen W, Fu Z, et al. MicroRNAs, a subpopulation of regulators, are involved in breast cancer progression through regulating breast cancer stem cells (Review). *Oncol Lett*. 2017;14(5):5069–5076. doi:10.3892/ol.2017.6867
7. [illegible] Zhang H, Duan CJ, et al. miR-675-5p enhances tumorigenesis and metastasis of esophageal squamous cell carcinoma by targeting REPS2. *Oncotarget*. 2016;7(21):30730.
8. Ishibashi O, Akagi I, Ogawa Y, et al. MiR-141-3p is upregulated in esophageal squamous cell carcinoma and targets pleckstrin homology domain leucine-rich repeat protein phosphatase-2, a negative regulator of the PI3K/AKT pathway. *Biochem Biophys Res Commun*. 2018;501(2):507–513. doi:10.1016/j.bbrc.2018.05.025
9. Jia Y, Lu H, Wang C, et al. miR-25 is upregulated before the occurrence of esophageal squamous cell carcinoma. *Am J Transl Res*. 2017;9(10):4458–4469.
10. Wang M, Wang L, Zhang M, et al. MiR-214 inhibits the proliferation and invasion of esophageal squamous cell carcinoma cells by targeting CDC25B. *Biomed Pharmacother*. 2017;95:1678–1683.
11. Cui XB, Peng H, Li RR, et al. MicroRNA-34a functions as a tumor suppressor by directly targeting oncogenic PLCE1 in Kazakh esophageal squamous cell carcinoma. *Oncotarget*. 2017;8(54):92454–92469.
12. Zheng S, Zhang X, Wang X, et al. Downregulation of miR-138 predicts poor prognosis in patients with esophageal squamous cell carcinoma. *Cancer Biomark*. 2017;20(1):49–54. doi:10.3233/CBM-170079
13. Luan W, Qian Y, Ni X, et al. miR-204-5p acts as a tumor suppressor by targeting matrix metalloproteinases-9 and B-cell lymphoma-2 in malignant melanoma. *Onco Targets Ther*. 2017;10:1237–1246. doi:10.2147/OTT.S128819
14. Chu Y, Jiang M, Du F, et al. MiR-204-5p suppresses hepatocellular cancer proliferation by regulating homeoprotein SIX1 expression. *FEBS Open Bio*. 2018;8(2):189–200. doi:10.1002/2211-5463.12363
15. Nishimura Y, Komatsu S, Ichikawa D, et al. Overexpression of YWHAZ relates to tumor cell proliferation and malignant outcome of gastric carcinoma. *Br J Cancer*. 2013;108(6):1324–1331. doi:10.1038/bjc.2013.65
16. Yin Y, Zhang B, Wang W, et al. miR-204-5p inhibits proliferation and invasion and enhances chemotherapeutic sensitivity of colorectal cancer cells by downregulating RAB22A. *Clin Cancer Res*. 2014;20(23):6187–6199. doi:10.1158/1078-0432.CCR-14-1030

17. Liu L, Wang J, Li X, et al. miR-204-5p suppresses cell proliferation by inhibiting IGFBP5 in papillary thyroid carcinoma. *Biochem Biophys Res Commun*. 2015;457(4):621–626. doi:10.1016/j.bbrc.2015.01.037
18. Wang X, Li F, Zhou X. miR-204-5p regulates cell proliferation and metastasis through inhibiting CXCR4 expression in OSCC. *Biomed Pharmacother*. 2016;82:202–207. doi:10.1016/j.biopha.2016.04.060
19. Lin M, Morrison CD, Jones S, et al. Copy number gain and oncogenic activity of YWHAZ/14-3-3zeta in head and neck squamous cell carcinoma. *Int J Cancer*. 2010;125(3):603–611.
20. Mao L, Zhang Y, Deng X, et al. Transcription factor KLF4 regulates microRNA-544 that targets YWHAZ in cervical cancer. *Am J Cancer Res*. 2015;5(6):1939–1953.
21. Watanabe N, Komatsu S, Ichikawa D, et al. Overexpression of YWHAZ as an independent prognostic factor in adenocarcinoma of the esophago-gastric junction. *Am J Cancer Res*. 2016;6(11):2729–2736.
22. Jiang X, Wu J, Zhang Y, et al. MiR-613 functions as tumor suppressor in hepatocellular carcinoma by targeting YWHAZ. *Gene*. 2018;659:S0378111918302749.
23. Li Y, Wang J, Dai X, et al. miR-451 regulates FoxO3 nuclear accumulation through Ywhaz in human colorectal cancer. *Am J Transl Res*. 2016;7(12):2775–2785.
24. Fang Y, Shen H, Cao Y, et al. Involvement of miR-30c in resistance to doxorubicin by regulating YWHAZ in breast cancer cells. *Braz J Med Biol Res*. 2014;47(1):60–69. doi:10.1590/1414-431X20133324
25. Chen M, Hu W, Xiong C-L, et al. miR-22 targets YWHAZ to inhibit metastasis of hepatocellular carcinoma and its down-regulation predicts a poor survival. *Oncotarget*. 2016;7(49). doi:10.18632/oncotarget.13037
26. Xie Q, Wen H, Zhang Q, et al. Inhibiting PI3K-Akt signaling pathway is involved in antitumor effects of ginsenoside Rg3 in lung cancer cell. *Biomed Pharmacother*. 2017;85:16–21. doi:10.1016/j.biopha.2016.11.096
27. Cheng F, Yang Z, Huang F, et al. microRNA-107 inhibits gastric cancer cell proliferation and metastasis by targeting PI3K/AKT pathway. *Microbial Pathogenesis*. 2018;121:110–114. doi:10.1016/j.micpath.2018.04.060
28. Fu X, Wen H, Jing L, et al. MicroRNA-155-5p promotes hepatocellular carcinoma progression by suppressing PTEN through the PI3K/Akt pathway. *Cancer Sci*. 2017;108(4):620–631. doi:10.1111/cas.13177
29. Sathe A, Nawroth R. Targeting the PI3K/AKT/mTOR pathway in bladder cancer. In: *Urothelial Carcinoma*. New York, NY:Humana Press; 2018:335–350.
30. Wang H, Yang X, Guo Y, et al. HERG1 promotes esophageal squamous cell carcinoma growth and metastasis through TXNDC5 by activating the PI3K/AKT pathway. *J Exp Clin Cancer Res*. 2019;38(1):324. doi:10.1186/s13046-019-1284-y
31. Chin YR, Toker A. The actin-bundling protein palladin is an Akt1-specific substrate that regulates breast cancer cell migration. *Mol Cell*. 2010;38(3):333–344. doi:10.1016/j.molcel.2010.02.031
32. Hui Wang, Cai J, Du S, et al. Fractalkine/CX3CR1 induces apoptosis resistance and proliferation through the activation of the AKT/NF-κB cascade in pancreatic cancer cells. *Cell Biochem Funct*. 2017;35(6):315–326.
33. Yang J, Zou Y, Yang D. Tanshinol suppresses proliferation and induces apoptosis via regulation of the miR-21/PTEN/PI3K/AKT signaling pathway in human osteosarcoma cells. *Int J Mol Med*. 2018;41:1845–1854.
34. Zhou S, Li J, et al. Effect of microRNA-135a on cell proliferation, migration, invasion, apoptosis and tumor angiogenesis through the IGF-1/PI3K/Akt signaling pathway in non-small cell lung cancer. *Cell Physiol Biochem*. 2017;42(4):1431–1446.